

## MODELLING OF COMBUSTION PROCESS OF LIQUID FUELS UNDER TURBULENT CONDITIONS

**Józef Żurek, Mirosław Kowalski**

*Air Force Institute of Technology*  
Ksiecica Bolesława Street 6, 01-494 Warsaw, Poland  
tel.: +48 22 6851300, fax: +48 22 6851300  
jozef.zurek@itwl.pl, miroslaw.kowalski@itwl.pl

**Antoni Jankowski**

*Institute of Aviation*  
Krakowska Avenue 110/114, 02-256 Warsaw, Poland  
tel.: +48 22 8460011, fax: +48 22 8464432  
e-mail: ajank@ilot.edu.pl

*Liquid fuel combustion model, taking into account washing out the fuel surface hot gas flow is presented. The laminar, transitional or turbulent flow exhaust gas stream takes place. This article refers to a turbulent flow. The model of the combustion process under turbulent flow conditions was used plane flow pattern. In the calculations of the turbulent flow was used two-dimensional turbulence model SST.*

*This model is a version of another model –  $k-\omega$ . The article presents the results of the velocity field (module with two velocity components), distribution of vector fields in a rectangular channel, flow lines, temperature distribution, velocity distributions and temperature. The article presents the results of the velocity field (module with two velocity components), distribution of vector fields in a rectangular channel, flow lines, temperature distribution, velocity distributions and temperature for different cross section, profile burnt samples - loss of burned mass on the sample, velocity distributions for particular sections for of the profile mass loss speed, temperature distribution for particular sections for each speed profile loss in mass of for turbulent flow with a Reynolds number  $Re = 3,550$ .*

*Developed theoretical combustion model has good reference for an experiment conducted in conditions of model confirmed using numerical and experimental studies of the boundary layer. The thickness of the laminar sublayer under turbulent flow conditions and laminar under laminar flow conditions have a significant impact on the course of the combustion process.*

**Keywords:** liquid fuels, combustion processes, turbulent flow, combustion process model, ANSYS FLUENT

### 1. Introduction

Depending on the kind of the exhaust gas flow, the laminar, transition or turbulent flow can take place. In [11, 14] experimental and numerical modelling of combustion process of liquid fuels under laminar conditions are presented. This article refers to a turbulent flow [2, 3, 4, 10]. There are many models of turbulence, the application of which depends on the course of events. In turbulent flows, models  $k-\epsilon$  and  $k-\omega$  are applied. With respect to the modelling, program ANSYS FLUENT [1] was used. This program provides modelling possibility of a wide range of problems associated with the calculation flow dynamics (CFD), both in relation to the flow of fluid compressible and incompressible, laminar flows and turbulent transport phenomena, heat exchange with the presence of and without the presence of chemical reactions. Particular emphasis on modelling such phenomenon presence during combustion is underlined, including models of energy dissipation and models of the probability density function.

With respect to all flows, using the code ANSYS FLUENT, the mass and momentum conservation equations can be resolved. The flows of heat exchange and the occurrence of compressibility, in addition to energy conservation equations should be included. Furthermore, in

regards to flows in which the mixing of the substances or chemical reactions occur, conservation equation particles or in the case of combustion model without mixing (non-premixed) conservation equation for the fraction of the mixture and the variances should be taken into account in [5, 6, 7].

Turbulent flows are characterized by the fluctuations of velocity fields. These fluctuations cause the mixing transport volumes, such as momentum, energy, concentration of particles and cause fluctuations of the transportation properties [12, 13]. Since these fluctuations occur on a small scale and high frequency, they can be resolved equations averaged over a time interval, or may be modified in such a way as to eliminate solutions to small-scale [8, 9]. The modified equations may include additional variables, and therefore it is necessary to introduce turbulence models to identify the variables in terms of known size. The modelling of the combustion process under turbulent flow conditions flat flow model is applied.

## 2. The modelling of complex turbulent flow in the channel

In [14], experimental and numerical modelling of combustion process of liquid fuels under laminar conditions relating to small values of the side velocity and low values of Reynolds number is presented. As the velocity increase the speed side of  $V_b$  up to 30 m/sec, it turns out that we get the flow for which the Reynolds number is 3,550. This means that the analysis of the case cannot use according to the laminar flow, and we need to use turbulent flow model.

### 2.1. Mathematical model

Turbulent flow model takes into account the averaged equations of conservation of mass, conservation of momentum and energy, which is described in research work (14).

The calculations assume the following values physicochemical parameters:

$$c_p = 1006.43 \frac{\text{J}}{\text{kg} \cdot \text{K}},$$

$$\lambda = 0.0242 \frac{\text{W}}{\text{m} \cdot \text{K}},$$

$$\mu = 1.7894e-5 \frac{\text{kg}}{\text{m} \cdot \text{s}},$$

where:

$c_p$  – specific heat capacity,

$\lambda$  – coefficient of heat conductivity,

$\mu$  – dynamic viscosity coefficient.

Turbulent flow model in addition to the averaged equations behaviour has the relationship between the components of the stress tensor of the turbulent fluid and physical properties [1]. In the calculations of the turbulent flow used in two-dimensional turbulence, model SST. This model is a variant of another model –  $k-\omega$ . During numerical calculations, two equations (1, 2) were solved:

$$\frac{\partial(\rho k \bar{u})}{\partial x} + \frac{\partial(\rho k \bar{v})}{\partial y} = \frac{\partial}{\partial x} \left( \Gamma_k \frac{\partial k}{\partial x} \right) + \frac{\partial}{\partial y} \left( \Gamma_k \frac{\partial k}{\partial y} \right) + \hat{G}_k - Y_k, \quad (1)$$

$$\frac{\partial(\rho \omega \bar{u})}{\partial x} + \frac{\partial(\rho \omega \bar{v})}{\partial y} = \frac{\partial}{\partial x} \left( \Gamma_\omega \frac{\partial \omega}{\partial x} \right) + \frac{\partial}{\partial y} \left( \Gamma_\omega \frac{\partial \omega}{\partial y} \right) + G_\omega - Y_\omega + D_\omega, \quad (2)$$

where:

$k$  – turbulence kinetic energy,

$\omega$  – turbulent kinetic energy dissipation rate,

$\hat{G}_k$  – generation of turbulent kinetic energy as a result of the average velocity gradient,

$G_\omega$  –  $\omega$  production,

$\Gamma_k, \Gamma_\omega$  – effective diffusion coefficients  $k$  and  $\omega$ ,

$Y_k, Y_\omega$  –  $k$  and  $\omega$  dissipation as a result of turbulence,

$D_\omega$  – lateral diffusion element.

The effective diffusion coefficient for the model SST  $k$ - $\omega$  is calculated from the relationship:

$$\Gamma_k = \mu + \frac{\mu_t}{\sigma_k}, \quad (3)$$

$$\Gamma_\omega = \mu + \frac{\mu_t}{\sigma_\omega}, \quad (4)$$

where:

$\sigma_k$  and  $\sigma_\omega$  – turbulent Prandtl number,  $\mu_t$  – turbulent dynamic viscosity coefficient, which is calculated from the relationship:

$$\mu_t = \frac{\rho k}{\omega} \frac{1}{\max\left[\frac{1}{\alpha^*}, \frac{SF_2}{\alpha_1 \omega}\right]}, \quad (5)$$

where:

$$\sigma_k = \frac{1}{\frac{F_1}{\sigma_{k,1}} + \frac{(1-F_1)}{\sigma_{k,2}}}, \quad (6)$$

$$\sigma_\omega = \frac{1}{\frac{F_1}{\sigma_{\omega,1}} + \frac{(1-F_1)}{\sigma_{\omega,2}}}, \quad (7)$$

$$S = \sqrt{2S_{ij}S_{ji}}, \quad (8)$$

where:

$S_{ij}$  – tensor components of deformation rate.

$$\alpha^* = \alpha_\infty^* \left( \frac{\alpha_0^* + \frac{Re_t}{R_k}}{1 + \frac{Re_t}{R_k}} \right), \quad (9)$$

$$Re_t = \frac{\rho k}{\mu \omega}, \quad (10)$$

where:

$$R_k = 6, \quad \alpha_0^* = \frac{\beta_i}{3}, \quad \beta_i = 0.072.$$

$$F_1 = \tanh(\Phi_1^4), \quad (11)$$

$$\Phi_1 = \min \left[ \max \left( \frac{\sqrt{k}}{0.09\omega y}, \frac{500\mu}{\rho y^2 \omega} \right), \frac{4\rho k}{\sigma_{\omega,2} D_\omega^+ y^2} \right], \quad (12)$$

$$D_\omega^+ = \max \left[ 2\rho \frac{1}{\sigma_{\omega,2}} \frac{1}{\omega} \frac{\partial k}{\partial x_j} \frac{\partial \omega}{\partial x_j}, 10^{-10} \right], \quad (13)$$

$$F_2 = \tanh(\Phi_2^2), \quad (14)$$

$$\Phi_2 = \max \left[ 2 \frac{\sqrt{k}}{0.09\omega y}, \frac{500\mu}{\rho y^2 \omega} \right]. \quad (15)$$

### 3. Modelling turbulence production

#### 3.1. Production $k$

Value of  $\widehat{G}_k$  represents the production of kinetic energy, which can be calculated from the equation (16).

$$\widehat{G}_k = \min(G_k, 10\rho\beta^*k\omega), \quad (16)$$

where:

$$G_k = -\rho\overline{u'_i u'_j} \frac{\partial u_j}{\partial x_i}. \quad (17)$$

#### 3.2. Production $\omega$

Element representing the production  $\omega$  can be calculated from equation (18).

$$G_\omega = \frac{\alpha}{\nu_t} \overline{G}_k, \quad (18)$$

where:

$$\alpha_\infty = F_1\alpha_{\infty,1} + (1-F_1)\alpha_{\infty,2}, \quad (19)$$

$$\alpha_{\infty,1} = \frac{\beta_{i,1}}{\beta_\infty^*} - \frac{\kappa^2}{\sigma_{\infty,1}\sqrt{\beta_\infty^*}}, \quad (20)$$

$$\alpha_{\infty,2} = \frac{\beta_{i,2}}{\beta_\infty^*} - \frac{\kappa^2}{\sigma_{\infty,2}\sqrt{\beta_\infty^*}}, \quad (21)$$

$\kappa = 0.41$ .

#### 3.3. Dissipation $k$

Element  $Y_k$  represents dissipation of turbulent kinetic energy, and it is defined by the equation (22).

$$Y_k = \rho\beta^*k\omega. \quad (22)$$

#### 3.4. Dissipation $\omega$

Element  $Y_\omega$  represents dissipation  $\omega$  and is defined by the equation (23).

$$Y_\omega = \rho\beta\omega^2, \quad (23)$$

$$\beta = F_1\beta_{i,1} + (1-F_1)\beta_{i,2}. \quad (24)$$

### 4. Transverse diffusion modification

Model SST is based on a standard model turbulence  $k$ - $\omega$  and  $k$ - $\varepsilon$ . To connect these two models, the standard model  $k$ - $\varepsilon$  converted into the equations of  $k$ - $\omega$ , which led to the Transverse diffusion element, which is defined by the relation (25).

$$D_\omega = 2(1-F_1)\rho\sigma_{\omega,2} \frac{1}{\omega} \frac{\partial k}{\partial x_j} \frac{\partial \omega}{\partial x_j}. \quad (25)$$

For the calculation, the following values of the constants are taken:

$$\begin{aligned} \sigma_{k,1} &= 1.176; & \sigma_{k,2} &= 1.0; & \sigma_{\omega,1} &= 2.0; & \sigma_{\omega,2} &= 1.168; \\ \alpha_1 &= 0.31; & \beta_{i,1} &= 0.075; & \beta_{i,2} &= 0.0828; \\ \alpha_\infty^* &= 1; & \alpha_\infty &= 0.52. \end{aligned}$$

### 5. The results of calculations for turbulent flow at $Re = 3,550$

For the flow of  $Re = 3,550$ , the calculation results are shown as graphs of velocity fields and temperature. The module with the velocity components depicted in the Fig. 1.

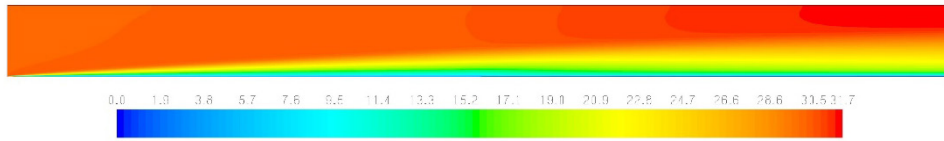


Fig. 1. Velocity field (module with two-component velocity) for the flow of  $Re = 3,550$

Graph of vector field is shown in Fig. 2.

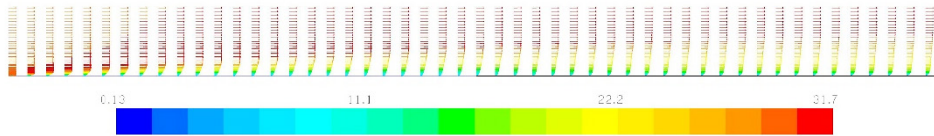


Fig. 2. Distribution of vector fields in the channel for the flow of  $Re = 3,550$

The flow lines and temperature distribution is shown in Fig. 3 and 4.

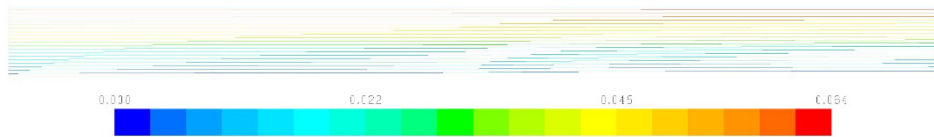


Fig. 3. The flow lines in the channel for  $Re = 3,550$

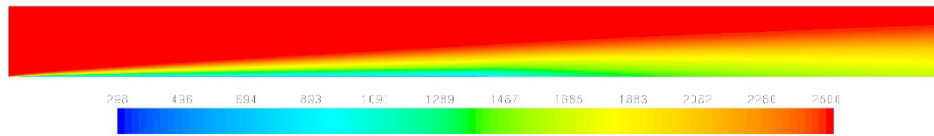


Fig. 4. Temperature distribution in the channel for  $Re = 3,550$

For the analysis of the hydraulic and thermal boundary layers, graphs are showing the velocity and temperature profiles at several cross-sections of the channel. As in previous laminar cases [14], the length of the analysed channel is divided into ten equal parts, and then interest distributions were defined. Distribution of velocity profile shown in Fig. 5.

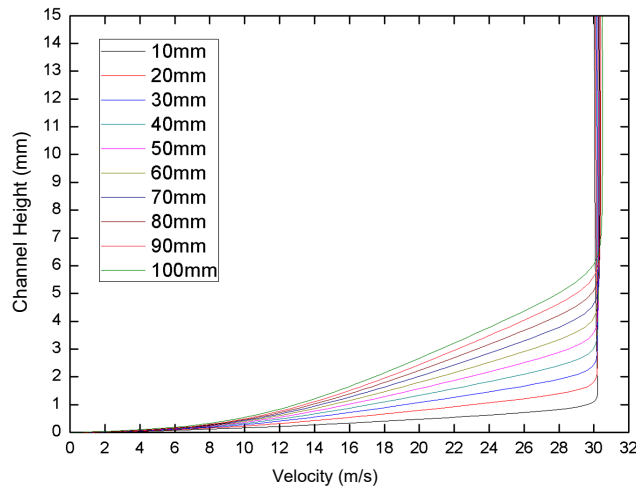


Fig. 5. Velocity distributions for each sections of channel for  $Re = 3,550$

Distribution of temperature profiles for the above flow is shown in Fig. 6.

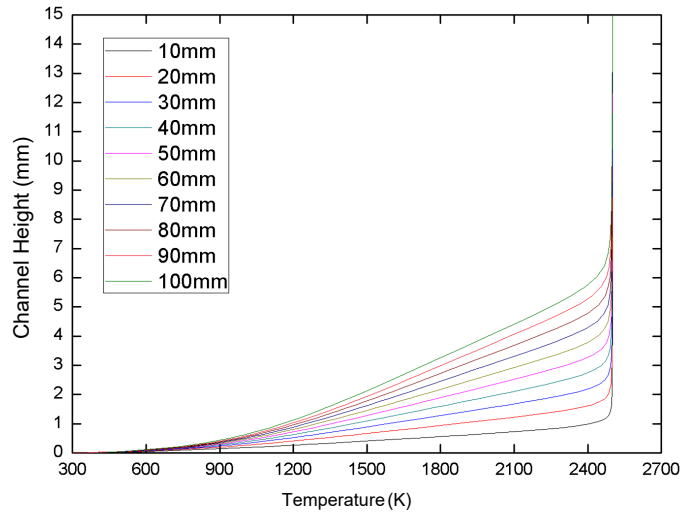


Fig. 6. Temperature distributions for each sections of channel for the flow of  $Re = 3,550$

Both profiles speed and breakdown temperatures are near the bottom of the wall, which indicates the presence of the laminar boundary sublayer. The Reynolds number was determined assuming that the entire channel is equal to the constant temperature of 2,500 K. However, due to the presence of cold air stream in the lower part of the channel, the average air temperature in the channel is lower. Knowing the temperature distribution, you can determine the average value of the medium temperature in the channel, and then adjust the calculations on the Reynolds number. The calculated average temperature is 1,709 K, which means that the Reynolds number was 5.193.

### 5. The results of calculations for the flow of $Re = 3,550$ , and with a fixed velocity profile $V_d$

Next simulation concerns the flow of steady velocity profile  $V_d$ . The calculation for this flow to be a model combustion of the sample in the channel with the flow of hot gases. In Figure 7a, the profile of the sample after a certain burning time is shown. Sample length is 100 mm. In the calculation model, the part that corresponds to the first part of the analysed channel. The loss of mass burned material suggests, what the burning rate distribution along burned samples is. It can be assumed that it is inversely proportional to mass loss. Calculations assume that it is linear. Profile flow rate  $V_d$ , which corresponds to the rate burning is shown in Fig. 7b.

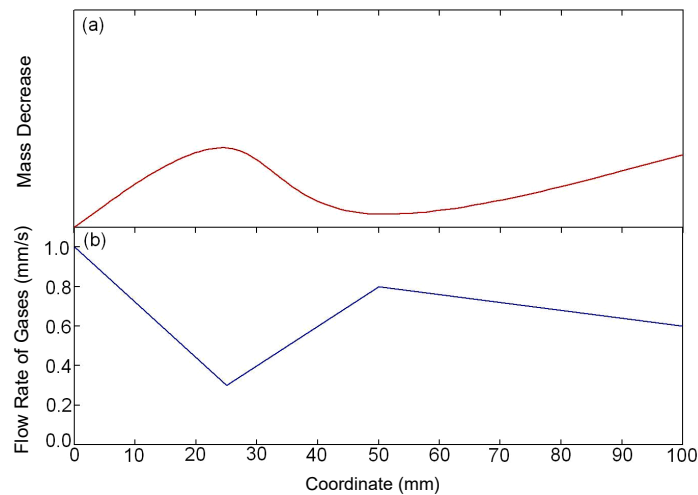


Fig. 7. Profile burned sample (a) established the velocity profile, (b) the loss of mass of the burnt sample

Obtained flow field simulation result is shown in Fig. 8.

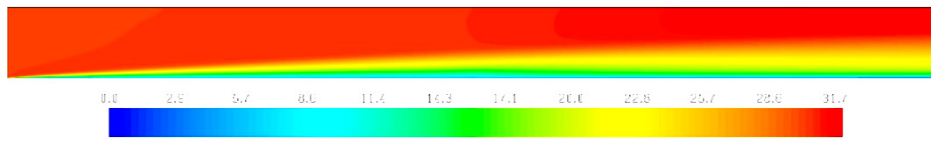


Fig. 8. Velocity field (modulus of two-component velocity) for the flow of  $Re = 3,550$ , and with a fixed velocity profile  $V_d$

Fig. 9 shows a graph of a vector field.

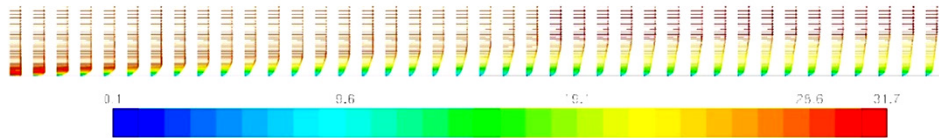


Fig. 9. The vector field distribution in the channel for the flow of  $e = 3.550$  and with a fixed velocity profile  $V_d$

Flow lines and temperature distribution are shown in Fig. 10 and 11.

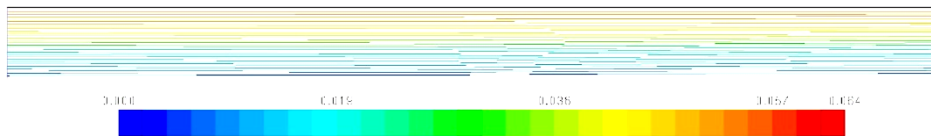


Fig. 10. The flow lines in the channel for flow with  $R = 3.550$  and with a fixed velocity profile  $V_d$

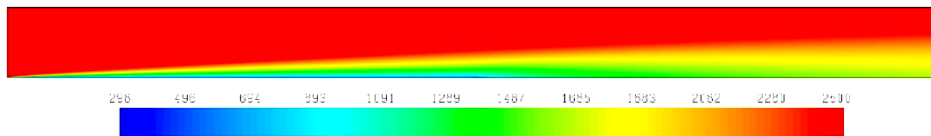


Fig. 11. The temperature distribution in the channel for the flow of  $Re = 3,550$  and with a fixed velocity profile  $V_d$

For analysed flow with  $Re = 3,550$  velocity and temperature profiles along the interesting part of the channel were determined. These are shown in Fig. 12 and 13.

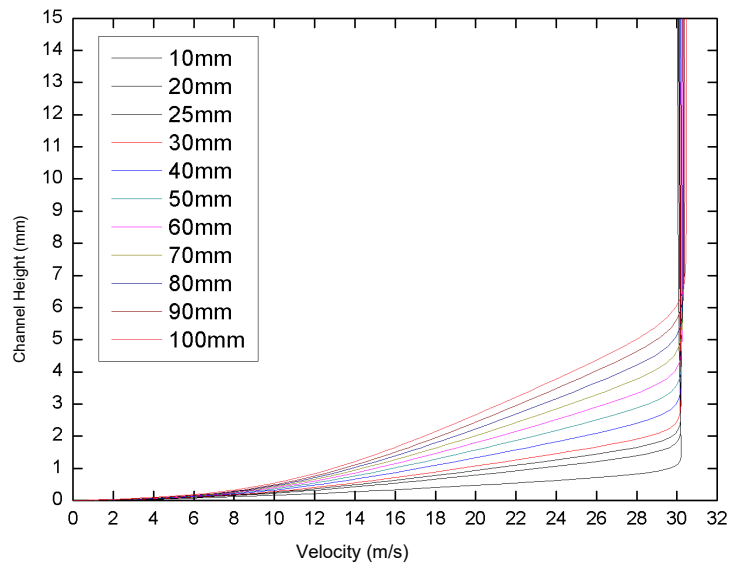


Fig. 12. Velocity distributions for each channel cross-sections for the flow with  $Re = 3,550$  for the velocity profile  $V_d$

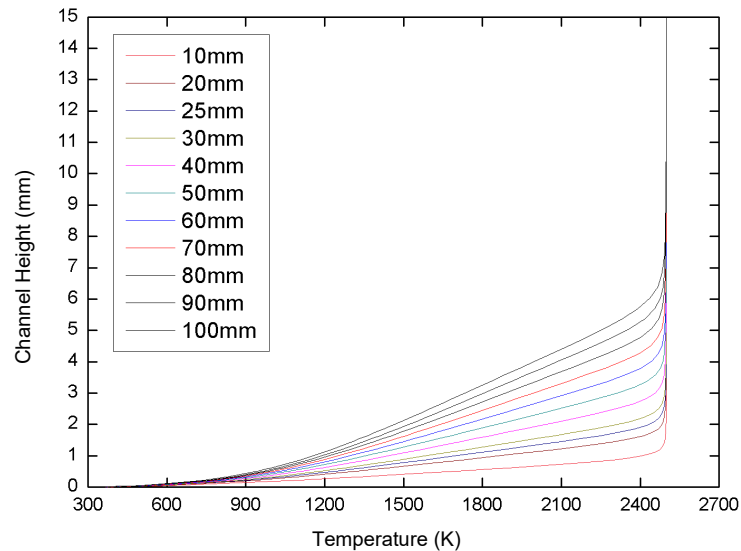


Fig. 13. Temperature distributions for each channel sections for the flow with  $R = 3,550$  and with a fixed velocity profile  $V_d$

## 6. Conclusions

The theoretical model of the combustion process relating to liquid fuels has been developed. It takes into account the influence of the gas phase, since combustion is always present in this phase, and interacts with the liquid phase. We found that the velocity gas stream and the type of flow (laminar, transitional, or turbulent) have a significant impact on the burning liquid fuels, and the impact of pressure always exists, which forces the gas stream. Developed a theoretical model burning has a good reference for an experiment conducted in conditions of model confirmed using numerical and experimental studies of the boundary layer.

The results of numerical calculations confirmed the presence of the laminar sublayer in the turbulent flow. The thickness of the sublayer laminar and turbulent flow conditions laminar under laminar flow conditions has a significant impact on the course of the combustion process. The use of a flat flow model reflects the basic phenomena that occur during combustion of liquid fuels in turbulent conditions.

In terms of turbulent flows basic relationship used in the modelling using ANSYS FLUENT were presented. Calculations for flows with different flow velocity profiles, modelling add mass and different values of module velocity were carried out. Velocity  $V_d$  modelling adding mass reflects the combustion process (adding mass to a stream of flowing gas).

In place of breakdown the characteristics of velocity  $V_d$  on the inlet is an evident increase in the velocity component  $V_y$  with very small changes of this component in the rest of the channel. In the case of a fault this area increased significantly, and the breakdown velocity is greater, the greater the disturbance component of the velocity field.

## References

- [1] *ANSYS FLUENT 12.0 Theory Guide*. 2009.
- [2] Gao J., Moon S., Zhang Y., Nishida K., Matsumoto Y., *Flame Structure of Wall Impinging Diesel Fuel Sprays Injected by Group-Hole Nozzles*, *Combustion and Flame*, Vol. 156, pp. 1263-1277, 2009.
- [3] Genzale, C. L., Reitz, R. D., Musculus, M. P. B., *Optical Diagnostics and Multi-Dimensional Modeling of Spray Targeting Effects in Late-Injection Low-Temperature Diesel Combustion*, *SAE International Journal of Engines*, Vol. 2, pp. 150-172, 2010.

- [4] Govardhan, J., Rao, G.V.S. *Influence of Oscillating Combustion on Thermal Boundary Layer in a Diesel Fired Crucible Furnace*, International Journal of Computer Information Systems and Industrial Management Applications, Vol. 2, pp. 056-068, 2010.
- [5] Jankowski, A., Czerwinski, J., *Memorandum of Prof. A. K. Oppenheim and an example of application of the Oppenheim correlation (OPC)\* for the heat losses during the combustion in IC-engine*, Journal of KONES, Vol. 17, No. 2, pp. 181-104, Warsaw 2010.
- [6] Jankowski, A., *Laser research of fuel atomization and combustion process in the aspect of exhaust gases emission*, Journal of KONES, Vol. 15, No. 1, pp. 119-126, 2008.
- [7] Jankowski, A., *Laser research of fuel atomization and combustion process in the aspect of exhaust gases emission*, Journal of KONES, Vol. 15, No. 1, pp. 119-126, Warsaw 2008.
- [8] Jankowski, A., *Laser Research of Fuel Atomization and Combustion Processes in the Aspect of Exhaust Gases Emission*, Journal of KONES, Vol. 15, No. 1 pp. 119-126, Warsaw 2008.
- [9] Jankowski, A., *Some Aspects of Heterogeneous Processes of the Combustion Including Two Phases*. Journal of KONES. Vol. 12, No. 1-2, pp. 121-134, Permanent Committee of KONES, Warsaw 2005.
- [10] Jankowski, A., *Study of the influence of pressure, speed and type of gas stream on the combustion process*, Scientific Papers of the Air Force Institute of Technology, Issue 28, (in Polish) Warsaw 2010.
- [11] Jankowski, A., *Test Stand for Modelling of Combustion Processes of Liquid Fuels*, Journal of KONES, Vol. 21, No. 2, pp. 121-126, 2014.
- [12] Kirchhartz, R. M., Mee, D. J., Stalker, R. J., *Effect of Boundary Layer Thickness and Entropy Layer on Boundary Layer Combustion*, 16th Australasian Fluid Mechanics Conference, Gold Coast, Australia, December 2007.
- [13] Xia, J., Luo, K. H., *Conditional Statistics of Inert Droplet Effects on Turbulent Combustion in Reacting Mixing Layers*, Combustion Theory and Modelling, Vol. 13, pp. 901-920, 2009.
- [14] Zurek, J., Jankowski, A., *Experimental and Numerical Modelling of Combustion Process of Liquid Fuels under Laminar Conditions*, Journal of KONES, Vol. 21. No. 3, pp. 30-316, Warsaw 2014.

